Average BER Analysis of NOMA Systems under TWDP Fading

Pawan Kumar
Department of Electronics and Communication Engineering
National Institute of Technology Rourkela
Rourkela, India
kumarpa@nitrkl.ac.in

Kalpana Dhaka
Department of Electronics and Electrical Engineering
Indian Institute of Technology Guwahati
Guwahati, India
kalpana.dhaka@iitg.ac.in

***Abstract*—This paper presents the average bit-error rate (BER) analysis of downlink non-orthogonal multiple access (NOMA) systems for binary phase-shift keying (BPSK) modulated data. The fading environment is considered to follow the two-wave with diffuse power (TWDP) distribution. The average BER expressions are analyzed for two-user and three-user NOMA systems using the moment generating function (MGF)-based method. Data detection at the users is done using the successive interference cancellation (SIC) method. The deduced analytical expressions are used to show the effects of variation in fading parameter values on the systems' performance. The simulation results are shown that validate the analytical outcome.**

Keywords – **Average bit-error rate (BER), NOMA, TWDP fading, 5G and Beyond.**

I. Introduction

From the first generation (1G) through the fourth generation (4G) mobile networks, users get services with the adoption of orthogonal multiple access (MA) techniques, namely, frequency division MA (FDMA), time division MA (TDMA), code division MA (CDMA), orthogonal frequency division MA (OFDMA), or space division MA (SDMA). The fifth generation (5G) and beyond 5G networks target to achieve immense connectivity (millions of devices per kilometer square area), data rates well above one gigabits per second (Gbps), latency less than one millisecond [1], [2]. People from both academia and industry are considering non-orthogonal MA (NOMA) technique as a strong candidate that can assist in meeting these requirements of the next-generation networks. In NOMA, multiple users can realize the transmission in power-domain, sparse-coding, and other domains [1].

Most of the works existing in the literature on the performance of NOMA systems have considered an information-theoretic approach. The outage probability, throughput, and ergodic capacity are analyzed in [3], [4]. Communication-theoretic analysis in terms of error-rates has recently found the interest of various group of researchers [5]- [9]. This paper aims to investigate error-rate performance of NOMA systems operating in power-domain, which is an usual consideration in the literature.

A. Literature Review

The authors in [5] investigated the average bit-error rate (BER) of uplink NOMA system for M-ary quadrature amplitude modulation (M-QAM) data. The analysis is provided for an arbitrary number of users under the Rayleigh fading environment. Subsequently, the authors in [6] considered an uplink two-user NOMA system and obtained the expressions for BER of quadrature phase-shift keying (QPSK) modulated data under additive white Gaussian noise (AWGN). In [7], the authors provided average BER analysis for a two-user uplink and downlink NOMA system under Rayleigh fading. It is considered that data of one user is QPSK modulated and that of the other user is binary PSK (BPSK) modulated. The performance of a two-user downlink NOMA system with M-QAM modulation under Rayleigh fading is examined in [8]. In [9] and [10], the average BER is analyzed under Nakagami-m fading channels. The authors in [9] provided analysis for a downlink two-user NOMA system assuming data are modulated using the BPSK scheme. Whereas, the authors in [10] considered the QPSK modulation scheme for two-user and three-user downlink NOMA systems. The average BER analysis under generalized κ–μ fading is presented in [11] for a cluster-based two-user downlink NOMA system.

κ-μ fading is a generalized scenario which includes classical fading models, namely, Rayleigh, Rician, Nakagami-m, etc. as special cases. Moreover, it emulates practical channel conditions in satellite communications, body-area networks, etc. [11]. However, this generalized fading model, including the classical fading models, is a cluster-based model which considers rich-scattering environment where multipaths of the transmitted signal arrive at the receiving end in cluster form. Such models fail to capture the channel's conditions at high frequency transmissions, particularly, in mmWave, terahertz, and visible light spectra [12]. The mmWave spectrum allows to achieve high data rate in 5G networks, while terahertz and visible light spectra are key elements for beyond 5G networks.

B. Motivation and Contribution

The fading models, namely, two-wave with diffuse power (TWDP), α-μ, and fluctuating two-ray (FTR) fading are considered to be a good approximation of mmWave and terahertz links [13] - [15]. In [16], sum-rate, outage probability, and ergodic capacity of a two-user downlink NOMA system is examined under FTR fading. The authors in [17] analyzed the average symbol-error rate for two-user cooperative NOMA

under TWDP considering QPSK and BPSK modulations.

The error-rate analysis in [5] - [11] is limited to two-user or three-user NOMA systems under the classical fading channels. The work in [17] considers two-user NOMA under TWDP fading. Recently, the authors in [18] and [19] investigated the BER of downlink NOMA system for arbitrary number of users. The Rayliegh fading environment and M-QAM scheme are considered for the analysis.

This paper aims to analyze the average BERs of downlink NOMA systems for two and three users under TWDP fading channel. The analytical results obtained are validated by simulations.

II. System model

We consider a downlink NOMA communication where a base station (BS) provides services to N number of users. Each communicating node is equipped with a single antenna. The BS superimposes data of all the users in power-domain and then broadcasts the superimposed signal. The superimposed signal can be represented as

$$x = \sum_{n=1}^{N} \sqrt{P_n T} s_n, \tag{1}$$

where $s_n \in \{-1, +1\}$ is BPSK modulated data of user U_n, $n \in \{1, 2\}$ for $N = 2$, $n \in \{1, 2, 3\}$ for $N = 3$, P_n is power assigned to user U_n, and T is transmission time. The energy consumed per transmission is $E_n = P_n T$, which for normalized time $T = 1$ can be given as $E_n = P_n$.

Fixed power allocation scheme is usually considered in NOMA systems. In this scheme, the power allocated to user U_n is calculated using the relation $P_n = \alpha P_{n-1}$ for $n > 2$, where $P_1 = P$ is power associated with the user U_1 which has the worst channel quality and the fraction $\alpha \in (0, 1)$ is used to assign power to other users. The power allocation to all the users is done at BS based on their link qualities. The channel state information (CSI) of all the links can be received at BS from the users in feedback path. Highest power is assigned to the user with worst link quality and lowest power to the user having the best channel condition. Let g_n represents the channel gain of BS-to-user U_n link which includes the effects of small scale fading and large scale fading. Let the BS decides the power variate of the channel gain in ascending order $|g_1|^2 < |g_2|^2 < \cdots < |g_N|^2$. Then the respective power allocated to all the users in descending order is given by $P_1 > P_2 > \cdots > P_N$. A larger fraction of power is assigned to the user having a smaller channel gain. The total transmit power can be obtained as $P_T = \sum_{n=1}^{N} P_n$.

The baseband equivalent of the received signal at user U_m, $1 \le m \le N$ is given by

$$\begin{aligned} r_m &= g_m x + \eta_m \\ &= \frac{h_m}{\sqrt{{d_m}^{\alpha_m}}} \left(\sum_{n=1}^{m-1} \sqrt{E_n} s_n + \sqrt{E_m} s_m + \sum_{n=m+1}^{N} \sqrt{E_n} s_n \right) + \eta_m, \end{aligned} \tag{2}$$

where $\eta_m \sim \mathcal{CN}(0, N_0)$ is zero-mean additive white Gaussian noise (AWGN) having power spectral density N_0, h_n is complex channel gain capturing the effects of small-scale fading, and ${d_n}^{\alpha_n}$ represent large-scale fading where d_n and α_n are distance between BS to user U_n and corresponding path loss exponent, respectively. We consider the communication happens in mmWave range and the small-scale fading of each link is modeled using TWDP fading.

Successive interference cancellation (SIC) is employed at the users for data detection. User U_m, for $1 \le m \le N$ first detects the data of users $U_1, U_2, \ldots, U_{m-1}$ successively and then use the detected data for cancellation. The received signal at user U_m can be expressed as

$$y_m = \frac{h_m}{\sqrt{{d_m}^{\alpha_m}}} \left(\sum_{n=1}^{m-1} \sqrt{E_n} \hat{\hat{s}}_n + \sqrt{E_m} s_m + \sum_{l=m+1}^{N} \sqrt{E_l} s_n \right) + \eta_m, \tag{3}$$

where $\hat{\hat{s}}_n \in \{-1, 1\}$ is a function of s_n and detected value of $\hat{s}_n$ for $1 \le n \le (m-1)$. Thus the decided bits can be correct or not is dependent on the correctness of SIC. Note that on SIC cancellation, $\hat{\hat{s}}_n$ corresponds to constellation points $-\sqrt{E_n}$ or $\sqrt{E_n}$ for the decided bits 0 or 1, respectively. Data detection for user U_m is done based on the decision variable $\Re\{h_m^* y_m\}$, thus the received instantaneous signal-to-noise (SNR) can be given as

$$\gamma_m = |h_m|^2 {\mathcal{E}_N}^2 / ({d_m}^{\alpha_m} N_0), \tag{4}$$

where $\mathcal{E}_N = \left(\sum_{n=1}^{m-1} \sqrt{E_n} \hat{\hat{s}}_n + \sqrt{E_m} s_m + \sum_{l=m+1}^{N} \sqrt{E_l} s_l \right)$. The probability density function (PDF) of the power variate $|h_m|^2$ for TWDP fading is given as [21]

$$f_{|h_m|^2}(x) = \sum_{p=0}^{\infty} \frac{{K_m}^p t_{m,p} x^p \exp(-K_m - x/(2{\sigma_m}^2))}{p! \Gamma(p+1) (2{\sigma_m}^2)^{p+1}}, \tag{5}$$

where

$$t_{m,p} = \sum_{q=0}^{p} \binom{p}{q} \left(\frac{\Delta_m}{2} \right)^q \sum_{r=0}^{q} \binom{q}{r} I_{2r-q}(-K_m \Delta_m)$$

and $K_m > 0$, $\Delta_m \in [0, 1]$, and $\sigma_m^2 > 0$ are fading parameters of the link connecting user U_m [21]. Using (4) and (5), the PDF of instantaneous SNR γ_m can be derived. This PDF is used in the next section for the average BER analysis.

III. Average BER Analysis

In this section, the average BER expressions are derived for 2-user NOMA and 3-user NOMA systems.

A. Average BER analysis for two-user NOMA

Fig. 1 depicts the constellation space and decision boundaries for users U_1 and U_2 in case of a two-user NOMA system. Using BPSK modulation for both the users, there are four constellation points after superimposition, Fig. 1(a). Let b_1 and b_2 correspond to information bits of users U_1 and U_2, respectively. The superimposed symbol is $b_1 b_2$. Here, bit b_1 is communicated with energy E_1 and bit b_2 with energy E_2. Thus on constellation diagram the constellation points for bit b_2 are located at distances $-\sqrt{E_2}$ and $+\sqrt{E_2}$ around the points for bit b_1. Without superimposition b_1 is placed at distances $-\sqrt{E_1}$ and $+\sqrt{E_1}$ around origin.

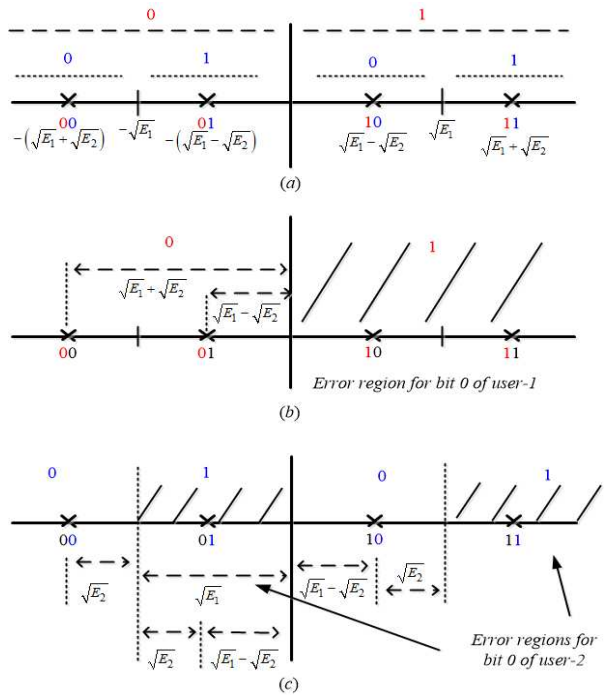

Fig. 1. Two-user NOMA. (a) Constellation space, (b) Decision boundaries for user U_1, (c) Decision boundaries for user U_2.

Using (3), the signal received at user U_1 can be written as

$$y_1 = \left(\sqrt{E_1}s_1 + \sqrt{E_2}s_2\right)h_1/\sqrt{{d_1}^{\alpha_1}} + \eta_1\,. \tag{6}$$

User U_1 detects its data considering the contribution from user U_2 as interference. SIC is performed at user U_2, where the data of user U_1 is detected first and then the detected data is scaled and subtracted from the received signal. The resultant signal for U_2's data detection can be written as (3)

$$y_2 = \left(\sqrt{E_1}\hat{\hat{s}}_1 + \sqrt{E_2}s_2\right)h_2/\sqrt{{d_2}^{\alpha_2}} + \eta_2\,. \tag{7}$$

Let Pe_{0,U_n} and Pe_{1,U_n} represent error probability at user U_n for bits $b_n = 0$ and $b_n = 1$, respectively. Considering bits 0's and 1's are transmitted with equal a priori probabilities, we have $Pe_{0,U_n} = Pe_{1,U_n}$. Hence the BER for user U_n can be given by

$$Pe_{U_n} = \frac{1}{2}(Pe_{0,U_n} + Pe_{1,U_n}) = Pe_{0,U_n}\,. \tag{8}$$

The error region for bit $b_1 = 0$ lies right to the origin as seen in Fig. 1(b). We have $b_1 = 0$ in two superimposed symbols, $b_1b_2 = 00$ and $b_1b_2 = 01$. The distance to decision boundary from these symbols are $(\sqrt{E_1} + \sqrt{E_2})$ and $(\sqrt{E_1} - \sqrt{E_2})$, respectively. Hence, the BER of bit $b_1 = 0$ can be given as

$$\begin{aligned}Pe_{U_1} =& \Pr[\Re\{h_1^* y_1\} > 0]\\ =& \frac{1}{2}\left(\Pr\left[\Re\left\{-\frac{|h_1|^2(\sqrt{E_1}+\sqrt{E_2})}{\sqrt{d_1^{\alpha_1}}} + h_1^*\eta_1\right\} > 0 | b_2 = 0\right]\right.\\ &\left. + \Pr\left[\Re\left\{-\frac{|h_1|^2(\sqrt{E_1}-\sqrt{E_2})}{\sqrt{d_1^{\alpha_1}}} + h_1^*\eta_1\right\} > 0 | b_2 = 1\right]\right)\\ =& \frac{1}{2}\int_0^\infty \frac{1}{\sqrt{\pi|h_1|^2N_0}}\exp\left(-\frac{\left(t + \frac{|h_1|^2(\sqrt{E_1}+\sqrt{E_2})}{\sqrt{d_1^{\alpha_1}}}\right)^2}{|h_1|^2N_0}\right)\\ &+ \frac{1}{2}\int_0^\infty \frac{1}{\sqrt{\pi|h_1|^2N_0}}\exp\left(-\frac{\left(t + \frac{|h_1|^2(\sqrt{E_1}-\sqrt{E_2})}{\sqrt{d_1^{\alpha_1}}}\right)^2}{|h_1|^2N_0}\right), \end{aligned}\tag{9}$$

where the integral representation follows from the fact that the decision variable $\Re\{h_1^* y_1\}$ has mean $-|h_1|^2(\sqrt{E_1}\pm\sqrt{E_2})/\sqrt{d_1^{\alpha_1}}$ and variance $|h_1|^2N_0/2$. The integrals in (9) can be expressed in the terms of Q-function as

$$Pe_{U_1} = \frac{1}{2}\left(Q\left(\sqrt{2\gamma_{1,1,00}}\right) + Q\left(\sqrt{2\gamma_{1,2,01}}\right)\right)\,, \tag{10}$$

where $\gamma_{1,\ell,0b_2} = |h_1|^2c_\ell^2/(d_1^{\alpha_1}N_0)$, $\ell = \{1,2\}$, $b_2 = \{0,1\}$, $c_{1,00} = (\sqrt{E_1}+\sqrt{E_2})$, and $c_{2,01} = (\sqrt{E_1}-\sqrt{E_2})$.

The error regions for $b_2 = 0$ are depicted in Fig. 1(c). It is worth to note here that due to symmetry of the constellation space, the error probability for $b_2 = 0$ in the entire plane is same as that of $b_2 = 0$ and $b_2 = 1$ in the left half of the plane. Hence, the BER of user U_2 can be given as

$$Pe_{U_2} = \frac{1}{2}\left(Pe_{2,00} + Pe_{2,01}\right)\,, \tag{11}$$

where $Pe_{2,00}$ and $Pe_{2,01}$ represent error probability for $b_1b_2 = 00$ and $b_1b_2 = 01$, respectively at U_2. Using Fig. 1(c) and following the steps adopted in (9) and (10), we have

$$Pe_{2,00} = \sum_{\ell=1}^{3}(-1)^{\ell-1}Q\left(\sqrt{2\gamma_{2,\ell,00}}\right) \tag{12}$$

and

$$Pe_{2,01} = \sum_{\ell=1}^{3}(-1)^{\ell-1}Q\left(\sqrt{2\gamma_{2,\ell,01}}\right)\,, \tag{13}$$

where $\gamma_{2,\ell,00} = |h_2|^2a_{\ell,00}^2/(d_2^{\alpha_2}N_0)$ for $\ell = \{1,2,3\}$, $\gamma_{2,\ell,01} = |h_2|^2\ a_{\ell,01}^2/(d_2^{\alpha_2}N_0)$ for $\ell = \{1,2\}$, $\gamma_{2,3,01} = |h_2|^2b_{1,01'}^2/(d_2^{\alpha_2}N_0)$. Here $a_{1,00} = \sqrt{E_2}$, $a_{2,00} = (\sqrt{E_1}+\sqrt{E_2})$, $a_{3,00} = (2\sqrt{E_1}+\sqrt{E_2})$, $a_{1,01} = (\sqrt{E_1}-\sqrt{E_2})$, $a_{2,01} = (2\sqrt{E_1} - \sqrt{E_2})$, and $b_{1,01'} = \sqrt{E_2}$. For $b_1b_2 = 00$, the distance of decision boundaries from the symbol are $a_{1,00}$, $a_{2,00}$, and $a_{3,00}$ in the rightward direction. The region corresponding to $b_1b_2 = 10$ provides correct detection, hence the term corresponding to $a_{2,00}$ is subtracted in (12). For $b_1b_2 = 01$, the decision boundaries are at distances $a_{1,01}$ and $a_{2,01}$ in rightward direction from the symbol and at distance $b_{1,01'}$ in the leftward direction (the notation $(')$ indicates the leftward direction). In this case, the region corresponding to $b_1b_2 = 11$ provides correct detection, hence the term corresponding to $a_{2,01}^2$ is subtracted in (13).

Substituting (12) and (13) in (11), we can obtain the BER for user U_2. The BER for user U_1 is given in (10). The BERs in (10) and (11) are conditioned on the varying channel gains $|h_1|^2$ and $|h_2|^2$. The corresponding average BER expressions

can be obtained by averaging (10) and (11) using the PDF in (5). Using Craig's result, the resulting BERs in the terms of integrals having integrands as products of $Q(\cdot)$ function and PDF of the instantaneous SNRs can be expressed in the terms of moment generating functions (MGFs) as

$$\bar{P}_{eU_1} = \frac{1}{\pi}\sum_{\ell=1}^{2}\int_0^{\pi/2} M_{\gamma_{1,\ell,0b_2}}\left(\frac{1}{\sin^2(\theta)}\right)d\theta \tag{14}$$

and

$$\bar{P}_{eU_2} = \frac{1}{\pi}\sum_{\ell=1}^{3}(-1)^{\ell-1}\int_0^{\pi/2} M_{\gamma_{2,\ell,00}}\left(\frac{1}{\sin^2(\theta)}\right)d\theta + \frac{1}{\pi}\sum_{\ell=1}^{3}(-1)^{\ell-1}\int_0^{\pi/2} M_{\gamma_{2,\ell,01}}\left(\frac{1}{\sin^2(\theta)}\right)d\theta\,, \tag{15}$$

respectively. The MGF of the instantaneous SNRs $\gamma_{m,\ell,0b_2}$ for $m = \{1,2\}$, $\ell = \{1,2,3\}$, and $b_2 = \{0,1\}$ can be obtained using the relations $M_{\gamma_m}(s) = \int_0^\infty \exp(-s\gamma)f_\gamma(\gamma)d\gamma$ and equations (4) and (5) as

$$M_{\gamma_{m,\ell,0b_2}}(s) = \sum_{p=0}^{\infty}\frac{{K_m}^p t_{m,p}}{p!\exp(K_m)}\left(\frac{1}{1+2sd_{\ell,0b_2,r}{\sigma_m}^2}\right)^{p+1}, \tag{16}$$

where $d_{\ell,0b_2,r}$ is related to the constants $c_{\ell,00}, a_{\ell,0b_2}$, $b_{1,01'}$. $r = 0$ and $r = 1$ indicate rightward and leftward directions, respectively.

The integrals in (14) and (15) can be expressed using (16) as

$$\mathcal{I}_{\gamma_{m,\ell,0b_2}} = \int_0^{\pi/2} M_{\gamma_{m,\ell,0b_2}}\left(\frac{1}{\sin^2(\theta)}\right)d\theta = \sum_{p=0}^{\infty}\frac{{K_m}^p t_{m,p}}{p!\exp(K_m)}\int_0^{\pi/2}\left(\frac{\sin^2(\theta)}{\sin^2(\theta)+2d_{\ell,0b_2,r}{\sigma_m}^2}\right)^{p+1}d\theta. \tag{17}$$

Substituting $\cos^2(\theta) = t$, (17) can be rewritten as

$$\mathcal{I}_{\gamma_{m,\ell,0b_2}} = \sum_{p=0}^{\infty}\frac{{K_m}^p t_{m,p}(1+2d_{\ell,0b_2,r}{\sigma_m}^2)^{-p-1}}{2p!\exp(K_m)} \times\int_0^1\frac{t^{-1/2}(1-t)^{p+1/2}}{(1-t/(1+2d_{\ell,0b_2,r}{\sigma_m}^2))^{p+1}}dt. \tag{18}$$

Using [22, eq. (3)], (18) can be simplified as

$$\mathcal{I}_{\gamma_{m,\ell,0b_2}} = \sum_{p=0}^{\infty}\frac{{K_m}^p t_{m,p}(1+2d_{\ell,0b_2,r}{\sigma_m}^2)^{-p-1}}{2p!\exp(K_m)} \times B\left(\frac{1}{2},p+\frac{3}{2}\right){}_2F_1\left(p+1,\frac{1}{2};p+2,\frac{1}{1+2d_{\ell,0b_2,r}{\sigma_m}^2}\right), \tag{19}$$

where $B(x,y)$ is beta function and ${}_2F_1(a,b;c,z)$ is Gauss's hypergeometric function [22, eq. (3)].

The average BER expressions for users U_1 and U_2 can be deduced using (14), (15), and (19).

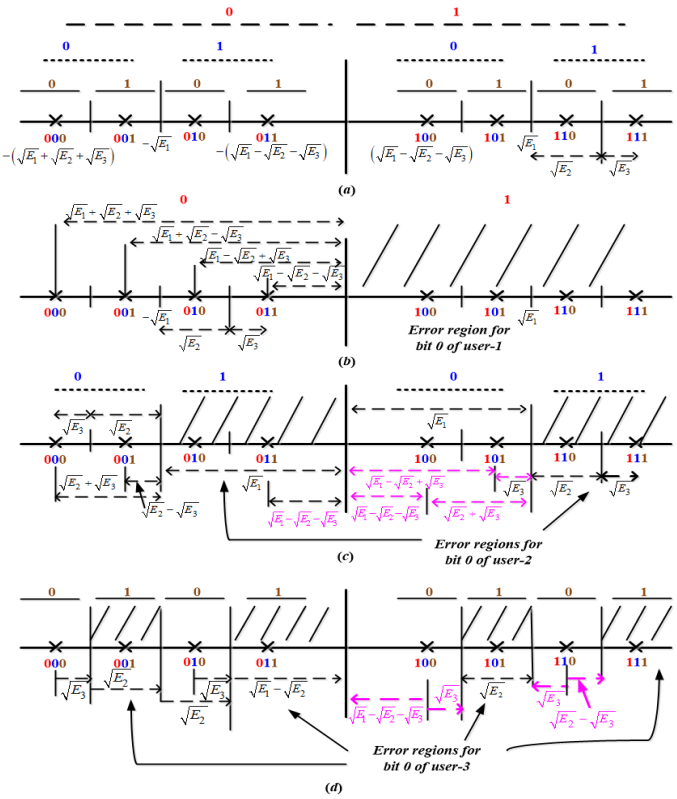

Fig. 2. Three-user NOMA. (a) Constellation space, (b) Decision boundaries for user U_1, (c) Decision boundaries for user U_2, (d) Decision boundaries for user U_3.

B. Average BER analysis for three-user NOMA

The constellation diagram for a three-user NOMA and the corresponding decision boundaries for users U_1, U_2, and U_3 are shown in Fig. 2. Using (3), the signals received at users U_1, U_2, and U_3 can be expressed as

$$y_1 = \frac{h_1}{\sqrt{{d_1}^{\alpha_1}}}\left(\sqrt{E_1}s_1+\sqrt{E_2}s_2+\sqrt{E_3}s_3\right)+\eta_1, \tag{20}$$

$$y_2 = \frac{h_2}{\sqrt{{d_2}^{\alpha_2}}}\left(\sqrt{E_1}\hat{s}_1+\sqrt{E_2}s_2+\sqrt{E_3}s_3\right)+\eta_2, \text{ and} \tag{21}$$

$$y_3 = \frac{h_3}{\sqrt{{d_3}^{\alpha_3}}}\left(\sqrt{E_1}\hat{s}_1+\sqrt{E_2}\hat{s}_2+\sqrt{E_3}s_3\right)+\eta_3, \tag{22}$$

respectively.

Following the procedure used for two-user NOMA in Section III-A, the BER for user U_1 can be obtained using Fig. 2(b) as

$$P_{e_{U_1}} = \frac{1}{4}\sum_{\ell=1}^{4}Q\left(\sqrt{2\gamma_{1,\ell,0b_2b_3}}\right), \tag{23}$$

where $b_2, b_3 \in \{0,1\}$, $\gamma_{1,\ell,0b_2b_3} = |h_1|^2\, c_{\ell,0b_2b_3}^2/(d_1^{\alpha_1}N_0)$ for $\ell = \{1,2,3\}$. Here $c_{1,000} = \sqrt{E_1}+\sqrt{E_2}+\sqrt{E_3}$, $c_{1,001} = \sqrt{E_1}+\sqrt{E_2}-\sqrt{E_3}$, $c_{1,010} = \sqrt{E_1}-\sqrt{E_2}+\sqrt{E_3}$, and $c_{1,011} = \sqrt{E_1}-\sqrt{E_2}-\sqrt{E_3}$. Similarly, with the help of Fig. 2(c), the error probability for user U_2 data can be given by

$$Pe_{U_2} = \frac{1}{4}\left(Pe_{2,000}+Pe_{2,001}+Pe_{2,010}+Pe_{2,011}\right), \tag{24}$$

where $Pe_{2,000}$, $Pe_{2,001}$, $Pe_{2,010}$, and $Pe_{2,011}$ represent probability of bit b_2 in error for $b_1b_2b_3 = 000$, 001, 010, and 011, respectively. Due to symmetry, we have $Pe_{2,010} = Pe_{2,101}$ and $Pe_{2,011} = Pe_{2,100}$. The terms in (24) can be expressed with the help of Fig. 2(c) as

$$Pe_{2,00b_3} = \sum_{\ell=1}^{3}(-1)^{\ell-1}Q\left(\sqrt{2\gamma_{2,\ell,00b_3}}\right) \text{ and } \quad (25)$$

$$Pe_{2,01b_3} = \sum_{\ell=1}^{3}(-1)^{\ell-1}Q\left(\sqrt{2\gamma_{2,\ell,01b_3}}\right), \quad (26)$$

where $b_3 = \{0,1\}$, $\gamma_{2,\ell,0b_2b_3} = |h_2|^2a^2_{\ell,0b_2b_3}/(d_2^{\alpha_2}N_0)$, $\gamma_{2,3,01b_3} = |h_2|^2b^2_{\ell,01b_3'}/(d_2^{\alpha_2}N_0)$, $a_{1,000} = \sqrt{E_2}+\sqrt{E_3}$, $a_{2,000} = \sqrt{E_1}+\sqrt{E_2}+\sqrt{E_3}$, $a_{3,000} = 2\sqrt{E_1}+\sqrt{E_2}+\sqrt{E_3}$, $a_{1,001} = (\sqrt{E_2}-\sqrt{E_3})$, $a_{2,001} = (\sqrt{E_1}+\sqrt{E_2}-\sqrt{E_3})$, $a_{3,001} = (2\sqrt{E_1}+\sqrt{E_2}-\sqrt{E_3})$, $a_{1,010} = (\sqrt{E_1}-\sqrt{E_2}+\sqrt{E_3})$, $a_{2,010} = (2\sqrt{E_1}-\sqrt{E_2}+\sqrt{E_3})$, $b_{1,010'} = (\sqrt{E_2}-\sqrt{E_3})$, $a_{1,011} = (\sqrt{E_1}-\sqrt{E_2}-\sqrt{E_3})$, $a_{2,011} = (2\sqrt{E_1}-\sqrt{E_2}-\sqrt{E_3})$, and $b_{1,011'} = (\sqrt{E_2}+\sqrt{E_3})$.

Similarly, using Fig. 2(d), the BER of user U_3 can be expressed as

$$Pe_{U_3} = \frac{1}{4}\left(Pe_{3,000}+Pe_{3,001}+Pe_{3,010}+Pe_{3,011}\right), \quad (27)$$

where $Pe_{3,000}$, $Pe_{3,001}$, $Pe_{3,010}$, and $Pe_{3,011}$ represent the probability of bit b_3 in error for $b_1b_2b_3 = 000$, 001, 010, and 011, respectively. Due to symmetry, we have $Pe_{3,001} = Pe_{3,110}$ and $Pe_{3,011} = Pe_{3,100}$. The term $Pe_{3,000}$ can be given as

$$P_{e_{3,000}} = \sum_{\ell=1}^{7}(-1)^{\ell-1}Q\left(\sqrt{2\gamma_{3,\ell,000}}\right), \quad (28)$$

where $\gamma_{3,\ell,000} = |h_3|^2a^2_{\ell,000}/(d_3^{\alpha_3}N_0)$. Here $a_{1,000} = \sqrt{E_3}$, $a_{2,000} = a_{1,000}+\sqrt{E_2}$, $a_{3,000} = a_{2,000}+\sqrt{E_2}$, $a_{4,000} = a_{3,000}+\sqrt{E_1}-\sqrt{E_2}$, $a_{5,000} = a_{4,000}+\sqrt{E_1}-\sqrt{E_2}$, $a_{6,000} = a_{5,000}+\sqrt{E_2}$, and $a_{7,000} = a_{6,000}+\sqrt{E_2}$. Similarly, the factor $Pe_{3,001}$ can be expressed as

$$Pe_{3,001} = \sum_{\ell=1}^{7}(-1)^{\ell-1}Q\left(\sqrt{2\gamma_{3,\ell,001}}\right), \quad (29)$$

where $\gamma_{3,\ell,001} = |h_3|^2a^2_{\ell,001}/(d_3^{\alpha_3}N_0)$ for $\ell = 1$ to 6, $\gamma_{3,7,001} = |h_3|^2b^2_{1,001'}/(d_3^{\alpha_3}N_0)$, $a_{1,001} = \sqrt{E_2}-\sqrt{E_3}$, $a_{2,001} = a_{1,001}+\sqrt{E_2}$, $a_{3,001} = a_{2,001}+\sqrt{E_1}-\sqrt{E_2}$, $a_{4,001} = a_{3,001}+\sqrt{E_1}-\sqrt{E_2}$, $a_{5,001} = a_{4,001}+\sqrt{E_2}$, $a_{6,001} = a_{5,001}+\sqrt{E_2}$, and $b_{1,001'} = \sqrt{E_3}$. Next, the factor $Pe_{0,010}$ is obtained as

$$Pe_{3,010} = \sum_{\ell=1}^{5}(-1)^{\ell-1}Q\left(\sqrt{2\gamma_{3,\ell,010}}\right) + \sum_{\ell=6}^{7}(-1)^{\ell}Q\left(\sqrt{2\gamma_{3,\ell,010'}}\right), \quad (30)$$

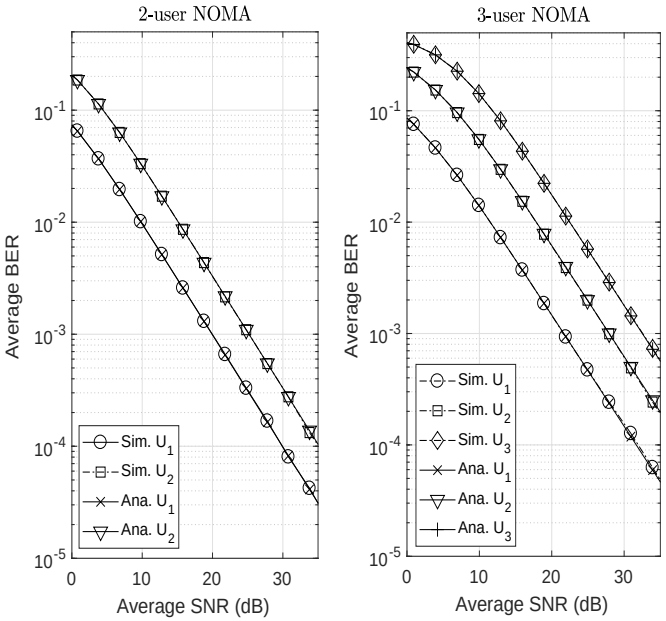

Fig. 3. Average BER versus average SNR plots for two-user and three-user NOMA systems. (Abbreviations: Sim. – Simulation, Ana. – Analytical)

where $\gamma_{3,\ell,010} = |h_3|^2a^2_{\ell,010}/(d_3^{\alpha_3}N_0)$ for $\ell = 1$ to 5, $\gamma_{3,\ell,010'} = |h_3|^2b^2_{\ell,010'}/(d_3^{\alpha_3}N_0)$ for $\ell = \{6,7\}$, $a_{1,010} = \sqrt{E_3}$, $a_{2,010} = a_{1,010}+\sqrt{E_1}-\sqrt{E_2}$, $a_{3,010} = a_{2,010}+\sqrt{E_1}-\sqrt{E_2}$, $a_{4,010} = a_{3,010}+\sqrt{E_2}$, $a_{5,010} = a_{4,010}+\sqrt{E_2}$, $b_{1,010} = \sqrt{E_2}-\sqrt{E_3}$, and $b_{2,010'} = b_{1,010}+\sqrt{E_2}$. Lastly, the factor $Pe_{3,011}$ is given by

$$Pe_{3,011} = \sum_{\ell=1}^{7}(-1)^{\ell-1}Q\left(\sqrt{2\gamma_{3,\ell,011}}\right), \quad (31)$$

where $\gamma_{3,\ell,011} = |h_3|^2a^2_{\ell,011}/(d_3^{\alpha_3}N_0)$ for $\ell = \{1,2,3,4\}$, $\gamma_{3,\ell,011} = |h_3|^2(b_{\ell,011'})^2/(d_3^{\alpha_3}N_0)$ for $\ell = \{5,6,7\}$, $a_{1,011} = \sqrt{E_1}-\sqrt{E_1}-\sqrt{E_2}$, $a_{2,011} = a_{1,011}+\sqrt{E_1}-\sqrt{E_2}$, $a_{3,011} = a_{2,011}+\sqrt{E_2}$, $a_{4,011} = a_{3,011}+\sqrt{E_2}$, $b_{1,011'} = \sqrt{E_3}$, $b_{2,011'} = b_{1,011}+\sqrt{E_2}$ and $b_{3,011'} = b_{2,011}+\sqrt{E_2}$. Substituting (28)-(31) in (27) produces the BER of user U_3.

The conditional BER expressions for the three users in (23), (24), and (27) can be used to derive the corresponding average BER expressions using the MGF-based approach as used in (14)-(19).

IV. Numerical Results

In this section, we present the average BER plots for a two-user and a three-user NOMA systems. The fixed power allocation fraction is taken as $P_{m-1}/P_m = 0.2$ for $m = 2,3,4$. The term 'average SNR' implies for the ratio P_T/N_0. The first 21 terms of the series in (16) are considered for calculating the analytical results.

In Fig. 3, plots are shown for the average BER of all users in a two-user NOMA and a three-user NOMA systems. Fading parameters $K_m = 1$ dB, $\Delta_m = 0.75$, and $\sigma_m^2 = 1$ are chosen. The effect of large-scale fading is normalized to unity, that is,

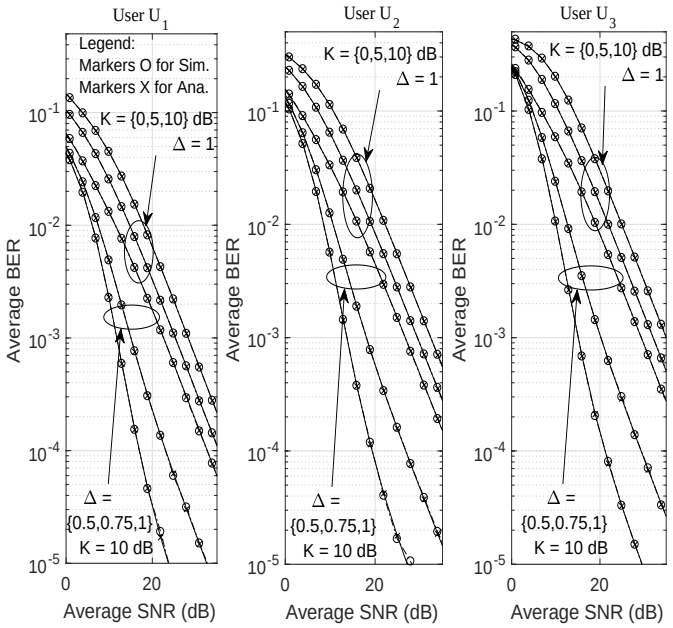

Fig. 4. Average BER versus average SNR plots for three-user NOMA system for fading parameters $\sigma_m = 1$, $K_m = \{0, 5, 10\}$ dB, and $\Delta_m = \{0.5, 0.75, 1.0\}$.

$(d_m)^{\alpha_m} = 1$. It is evident from the figure that the analytical results closely match with the simulated results for all the cases. This validates our analysis.

Fig. 4 shows the effects of variation in the average BER with fading parameters for a three-user NOMA system. For $\sigma_m^2 = 1$, two cases are considered: (i) $K = K_m = \{0, 5, 10\}$ dB when $\Delta = \Delta_m = 1$ and (ii) $\Delta = \{0.5, 0.75, 1.0\}$ when $K = 10$ dB. The results are shown for distances $d_1 = 1$ unit, $d_2 = 1.1 \times d_1$, and $d_3 = 1.2 \times d_1$. The path loss exponent is chosen as $\alpha = 3$. The figure suggests that the average BER decreases when there is an increment in K or decrement in Δ.

V. Conclusion

In this paper, the average BERs expressions of two-user and three-user NOMA systems are analyzed for BPSK modulated data under TWDP fading. The obtained analytical results are verified with the simulated results. The effect of the parameters of the TWDP faded channel are also observed. The system BER performance improves with increase in K or decrease in Δ. The possible future research direction from this work are a) extension to arbitrary number of users and b) extension to modulation orders M.

References

[1] M. Vaezi, Z. Ding, and V. Poor, *Multiple Access Techniques for 5G Wireless Networks and Beyond*. Cham, Switzerland:Springer, 2019.

[2] O. Maraqa, A.S. Rajasekaran, S. Al-Ahmadi, H. Yanikomeroglu, and S.M. Sait, "A survey of rate-optimal power domain NOMA with enabling technologies of future wireless networks," *IEEE Commun. Surv. Tut.*, vol. 22, no. 4, pp. 2192-2235, 4th-quarter 2020.

[3] A. A. Badrudeen, C. Y. Leow, and S. Won, "Performance analysis of hybrid beamforming precoders for multiuser millimeter wave NOMA systems," *IEEE Trans. Veh. Technol.*, vol. 69, no. 8, pp. 8739-8752, Aug. 2020.

[4] Y. Tian, G. Pan, and M.-S. Alouini, "On NOMA-based mmWave communications," *IEEE Trans. Veh. Technol.*, vol. 69, no. 12, pp. 15398-15411, Dec. 2020.

[5] H. Haci, H. Zhu, and J. Wang, "Performance of non-orthogonal multiple access with a novel asynchronous interference cancellation technique", *IEEE Trans. Commun.*, vol. 65, no. 3, pp. 1319-1335, Mar. 2017.

[6] X. Wang, F. Labeau, and L. Mei, "Closed-form BER expressions of QPSK constellation for uplink non-orthogonal multiple access," *IEEE Commun. Lett.*, vol. 21, no. 10, pp. 2242-2245, Oct. 2017.

[7] F. Kara and H. Kaya, "BER performances of downlink and uplink NOMA in the presence of SIC errors over fading channels,"*IET Commun.*, vol. 12, no. 15, pp. 1834-1844, Aug. 2018.

[8] T. Assaf, A. J. Al-Dweik, M. S. E. Moursi, H. Zeineldin, and M. Al-Jarrah, "Exact bit error-rate analysis of two-user NOMA using QAM with arbitrary modulation orders," *IEEE Commun. Lett.*, vol. 24, no. 12, pp. 2705-2709, Dec. 2020.

[9] M. Jain, S. Soni, N. Sharma, and D. Rawal, "Performance analysis at near and far users of a NOMA system over fading channels," in *Proc. IEEE 16th India Council Int. Conf. (INDICON)*, Rajkot, India, Dec. 13-15, 2019, pp. 1-5.

[10] T. Assaf, A. Al-Dweik, M. E. Moursi, and H. Zeineldin, "Exact BER performance analysis for downlink NOMA systems over Nakagami-m fading channels," *IEEE Access*, vol. 7, pp. 134539-134555, Sep. 2019.

[11] B. M. ElHalawany, F. Jameel, D. B. da Costa, U. S. Dias, and K. Wu, "Performance analysis of downlink NOMA systems over $\kappa - \mu$ shadowed fading channels," *IEEE Trans. Veh. Technol.*, vol. 69, no. 1, pp. 1046-1050, Jan. 2020.

[12] I. A. Hemadeh, K. Satyanarayana, M. El-Hajjar, and L. Hanzo, "Millimeter-wave communications: Physical channel models, design considerations, antenna constructions, and link-budget," *IEEE Commun. Surv. Tut.*, vol. 20, no. 2, pp. 870-913, 2nd-quarter 2018.

[13] T. S. Rappaport, R. W. Heath Jr., R. C. Daniels, and J. N. Murdock, *Millimeter Wave Wireless Communications*. Westford, Massachusetts, USA: Pearson Ed., 2015.

[14] A.-A. A. Boulogeorgos, E. N. Papasotiriou, and A. Alexiou, "Analytical performance assessment of THz wireless systems," *IEEE Access*, vol. 7, pp. 11436-11453, Jan. 2019.

[15] M. Bilim and N. Kapucu, "Average symbol error rate analysis of QAM schemes over millimeter wave fluctuating two-ray fading channels," *IEEE Access*, vol. 7, pp. 105746-105754, 2019.

[16] Y. Tian, G. Pan, and M.-S. Alouini, "On NOMA-based mmWave communications," *IEEE Trans. Veh. Technol.*, vol. 69, no. 12, pp. 15398-15411, Dec. 2020.

[17] R. Makkar, S. Soni, D. Rawal, N. Sharma, P. Garg, "Performance analysis of non-orthogonal multiple access assisted cooperative maritime communication system over two-wave with diffuse power fading," *Trans. Emerging Telecommunications Technol.*, vol. 33, no. 7, pp. 1-16, Feb. 2022.

[18] H. Yahya, E. Alsusa, and A. Al-Dweik, "Exact BER analysis of NOMA with arbitrary number of users and modulation orders," *IEEE Trans. Commun.*, vol. 69, no. 9, pp. 6330-6344, Sep. 2021.

[19] H. Semira, F. Kara, H. Kaya, and H. Yanikomeroglu, "Error performance analysis of multiuser detection in uplink-NOMA with adaptive M-QAM," *IEEE Wireless Commun. Lett.*, vol. 11, no. 8, pp. 1654-1658, Aug. 2022.

[20] M. Aldababsa, A. Khaleel, and E. Basar, "STAR-RIS-NOMA networks: An error performance perspective," *IEEE Commun. Lett.*, vol. 26, no. 8, pp. 1784-1788, Aug. 2022.

[21] N. Y. Ermolova, "Capacity analysis of two-wave with diffuse power fading channels using a mixture of gamma distributions," *IEEE Commun. Lett.*, vol. 20, no. 11, pp. 2245-2248, Nov. 2016.

[22] M. E. H. Ismail and J. Pitman,"Algebraic evaluations of some Euler integrals, duplication formulae for Appells hypergeometric function F1, Brownian variations," Department of Statistics, University of California, Berkeley, CA, USA, Tech. Rep., Aug. 1999, vol. 554.